

24 **INTRODUCTION**

25 The Hirnantian mass extinction (HME) is recognized as the first of the “Big Three,” and along
26 with the end- Permian and end- Cretaceous events results from an acceleration in biotic
27 extinctions concomitant with a rise in originations (Bambach et al., 2004). Estimates indicate
28 that in the marine realm 20% of families, 40% of genera (Sepkoski 1996) and by extrapolation
29 about 85% of marine species went extinct at this time (Jablonski 1991) , making the HME
30 second only in scale to the end-Permian in taxonomic impact. This extinction terminated the
31 Great Ordovician Biodiversification Event (GOBE) and was followed by the Paleozoic plateau in
32 biodiversity that continued until the end of the Paleozoic Era (Harper et al., 2013 in press).

33

34 **Figure 1 about here**

35

36 The HME is unusual in that, a) it is associated with glaciation, but there is little evidence
37 elsewhere in the Phanerozoic that glaciations have been a cause of mass extinction and, b) there
38 is limited understanding of how glaciation directly causes mass extinction, particularly in the
39 marine realm. Pleistocene sea level changes did not much affect the marine biosphere at any
40 ecological level (Valentine and Jablonski, 1991) and habitat tracking appears to have been an
41 important process in insulating the biosphere from mass extinction at this time (Brett et al.,
42 2007). Glacially-induced cooling, falling sea level and chemical recycling in the oceans are
43 three of the many suggested kill mechanisms for end-Ordovician extinction, but a general
44 consensus is lacking (Finnegan et al 2012; Harper et al., 2013 in press).

45

46 **Figure 2 about here**

47

48 The HME comprised two extinction phases which are known in some detail (e.g.,
49 (Brenchley and Cullen, 1984; Brenchley et al., 2006; Fig. 2). The “first strike”, occurred at or
50 just below, the *N. extraordinarius* graptolite biozone, and coincided with the onset of glaciation
51 and a fall in global sea level (Fig. 3). Continental ice was centred on the supercontinent of
52 Gondwana, located over the South Pole during the Late Ordovician (Brenchley and Cullen,
53 1984; Brenchley et al., 2001). During this phase, benthic organisms in deep and shallow-water
54 environments were more affected than organisms occupying mid-shelfal depths.
55 Planktonic/nektonic organisms, particularly graptolites, and nektonic groups, were differentially
56 more greatly affected (Rasmussen and Harper, 2011a, b and references herein). The second
57 strike, started at the base of the *N. persculptus* graptolite biozone, and coincided with a rise in
58 sea-level and the widespread deposition of black shale in continental shelf settings (Fortey,
59 1989). During this phase coordinated extinctions occurred across the mid- outer shelf and
60 particularly in mid-shelf settings.

61

62 **Figure 3 about here**

63

64 **Global climate context**

65 Estimates of the duration of the Hirnantian Glacial Maximum vary but may have been less than 1
66 myr (e.g. Armstrong, 2007; Holmden et al. 2012). A “short, sharp glaciation” cause for mass
67 extinction can now be re-evaluated against a better understanding of longer-term Ordovician
68 climate change and a large relatively new database of environmental proxies.

69 **Figure 4 about here**

70

71 Emerging new climate scenarios for the Ordovician indicate a modern “cool world” existed
72 from the Early Ordovician (~472Ma; Trotter et al.,2008; Vandenbroucke et al., 2009) with
73 successive glaciations during the Floian, Darriwilian, Katian (Guttenburg) and Hirnantian
74 (Turner et al., 2011; Turner et al., 2012). These occurred against a backdrop of long-term
75 declining $p\text{CO}_2$ (Godderis et al., 2001; Figs 4, 5) probably initiated by changes in plate
76 configuration that resulted in increased weathering and nutrient cycling into the oceans, changes
77 in volcanic outgassing of greenhouse gases and the re-direction of ocean currents. The rapid
78 expansion of ice volume, during successive intervals of Ordovician glaciation was triggered by
79 orbitally-induced cooling (Turner et al., 2011; Turner et al., 2012). During each glaciation the
80 Gondwana ice sheet grew large enough to be affected by eccentricity-pacing of ice margin
81 processes embedded in obliquity which largely controlled their size (Armstrong, 2007).
82 Composite $\delta^{13}\text{C}_{\text{carb}}$ records for the entire Ordovician show a long-term broadly positive trend
83 with increasingly large positive excursions through successive Ordovician glaciations
84 (Bergström et al., 2009; Fig. 5).

85

86 **Figure 5 about here**

87

88

89 Positive isotope excursions (base Floian, DICE, GICE and HICE) coincide with intervals
90 characterized by c. 1.2 myr long obliquity cycles, interpreted to indicate icehouse conditions
91 (Boulila et al., 2011; Turner et al., 2011; Turner et al., 2012; Fig. 5). The $\delta^{13}\text{C}$ data suggest an
92 ever-present Gondwana ice sheet that grew in a stepwise fashion to reach maximum size in the

93 Hirnantian. The Hirnantian Glaciation and associated mass extinction may thus be viewed as a
94 “tipping point” in the Earth surface system, when the polar ice sheet was large enough to have a
95 maximal effect on the ocean-atmosphere system (Armstrong, 2007).

96 **Biotic patterns during mass extinction**

97 *Pattern 1. High taxonomic impact but low ecological impact.*

98 No major taxonomic groups or trophic groups disappeared during the HME and the event
99 has been classified as being of high taxonomic impact but low ecological impact (Droser et al.,
100 2000; McGhee Jr et al., 2013). It is acknowledged that the Hirnantian biotic record is far from
101 complete, largely documented at the level of geological stage and biased towards continental
102 shelf settings in low paleo-latitudes. Despite this the patterns and trends of extinction are uneven
103 across continents but these are as yet poorly documented and understood (Harper and Rong,
104 2008). Despite this the uneven pattern of extinctions likely provided refugia during peak
105 glaciation as evidenced by a high proportion of Lazarus taxa (Brett et al., 2007; Rong et al.,
106 2006). The relatively rapid recovery of the major clades and their benthic communities indicate
107 minimal ecological disruption and largely within community species level extinction (Droser et
108 al., 2000); this is particularly well-demonstrated by tropical communities. Despite significant
109 global cooling, tropical bioherm communities remained largely unaffected by the HME and
110 rugose and tabulate corals continued to radiate into the Silurian (Fig. 6A). Bioherms expanded
111 rapidly during the Llandovery and went on to dominate many Silurian carbonate environments
112 but, these communities had similar taxonomic compositions, species richness and trophic
113 structure, to those of the Katian (Copper and Jin, 2012)

114

115 **Figure 6 about here**

116

117 ***Pattern 2. Variance in patterns of extinction between the benthic and pelagic realms.***

118 The phytoplankton, including the acritarchs (chromophyte algae) and in deeper
119 environments, cyanobacteria, formed the base of the food chain in Late Ordovician ecosystems.
120 (Servais et al., 2008). Patterns of diversity decline are similar in phytoplankton, zooplankton and
121 nektonic groups (Fig. 6B). All groups reach peak diversity in the late Darriwilian (Llandeilo)
122 and show declining diversity through the Late Ordovician, recovering at a variety of rates until
123 the mid- Silurian. The onset of diversity decline is significantly earlier than in benthic groups.
124 Acritarch species-richness declined dramatically from the late Darriwilian (Llandeilo), with a
125 similarly spectacular recovery in the Llandovery (Fig. 2, 6B). Chitinozoa and graptolites formed
126 the preserved zooplankton and both groups declined markedly in diversity during the first strike
127 of extinction. Graptolites were already in a state of decline from the Darriwilian (late Middle
128 Ordovician); the group was reduced to only a few genera and less than 20 species by the first
129 strike of the HME (Bapst et al., 2012). Graptolite disparity, as evidenced by a marked reduction
130 in the range of graptolite rhabdosome and theca morphologies, also decreased during the mass
131 extinction interval. However, many of the thecal morpho-types present in the Ordovician are
132 found in the Silurian monograptids, suggesting these were hydrodynamic adaptations as the
133 graptolites re-occupied specific niches (M. Williams pers comm., 2013) . Over 200 species have
134 been reported from the Upper Llandovery (Lower Silurian; Zalasiewicz et al. 2009).

135 Species distribution studies indicate graptolites lived in two primary depth zones of the
136 ocean waters. A shallow, epipelagic zone biotope contained species found preserved in all depth
137 facies, whereas a deep, mesopelagic, zone biotope contained species now found only in deep-
138 water facies (isograptid biofacies) (Cooper et al., 1991). Mesopelagic taxa thrived in continental-

139 margin upwelling zones and within the oxygen-minimum zone where their rhabdosomes were
140 preserved (Finney and Berry (1997). Epipelagic biotope species were affected by sea surface
141 temperature (see below). extinctions in the mesopelagic biotope are poorly constrained but
142 would have reflected oceanographic changes and feedbacks (especially upwelling and redox
143 conditions) that were driven by climatic and tectonic events (Finney and Berry 1997).

144 In the nekton, trilobites including the cyclopygids disappeared entirely. The top predators
145 of the Ordovician, the nautiloid cephalopods, were significantly reduced in diversity during the
146 extinction interval, from nearly 300 species at the height of the GOBE to some 50 during the
147 Hirnantian. This decline in diversity has been attributed to Early Hirnantian regression, draining
148 many of the epicontinental seas, and destroying habitats for potential prey (Harper et al., 2013 in
149 press).

150 In contrast, benthic groups, both sessile and motile, show diversity peaks at different times
151 (e.g. see papers in Webby et al. 2004) (Fig. 6A). Global analyses of Upper Ordovician and
152 Lower Silurian brachiopods indicate that 18.6% and 12.5% of families and 51.0% and 41.3% of
153 genera were eliminated in the first and second phases of the mass extinction, respectively, with
154 the total loss of 28.4% of families and 69.0% of genera in the crisis (Rong et al., 2006).

155 Although various major groups of brachiopods suffered substantially during the extinction, there
156 was clearly phylogenetic and ecological continuity between the Late Ordovician and Early
157 Silurian shelf faunas (Droser et al., 1997). The extinction of brachiopods did not cease at the
158 HME with a relict Ordovician association. Evidence from the Oslo Region and South China
159 suggests that part of the initial Silurian fauna consisted of the more eurytopic taxa of the
160 regressive succession that survived the extinction in the deeper parts of the intracratonic basin
161 (e.g. Baarli and Harper, 1986; Rong and Zhan, 2006; Owen et al. 2008). These species were

162 subsequently able to create and participate within new community structures during the Early
163 Silurian transgression (Rong and Harper, 1999).

164 Through the HME trilobites suffered losses in the region of 70% at the generic level, and
165 all unequivocally pelagic taxa became extinct by the end of the HME. Of the main trophic
166 groups the filter feeders were differentially affected but did not disappear and these changes had
167 little effect on the overall community structure (Adrain et al., 2004). In detail there is a marked,
168 two-stage reduction in diversity at the base of the *N. extraordinarius* and *N. persculptus*
169 graptolite biozones (Brenchley et al., 2001; see below). Benthic taxa that survived the first phase
170 of extinction commonly succumbed to the second.

171

172 ***Pattern 3. Extinctions in the epipelagic zone were associated with a narrowing of temperature***
173 ***defined provinces***

174

175 **Figure 7 abut here**

176

177 Biogeographical provinces are aggregations of communities and their number and
178 individual compositions affect global or gamma biodiversity levels. Today temperature is the
179 most important factor in defining the boundaries of biogeographical provinces that broadly
180 follow the climate belts in the marine realm (Kucera 2007) . Paleobiogeographical studies of
181 epipelagic organisms through the Late Ordovician indicate that during the Hirnantian Glaciation
182 the latitudinal temperature gradient steepened and provinces shifted equator-wards
183 (Vandenbroucke et al., 2010a; Vandenbroucke et al., 2010b; Fig. 7). These data suggest the
184 geographical extent of the Tropical Province remained largely unaffected by the change from

185 inter-glaciation (Sandbian distribution) to Hirnantian glaciation. The low-diversity Polar
186 Province expanded in geographical extent. Extinction was highest in the more diverse Subpolar
187 Province, associated with the narrowing of the zone (Vandenbroucke et al., 2010a).

188 A link between species richness and provinciality is also recognized in brachiopods.
189 Sheehan and Coorough (1990) recognised ten Katian brachiopod provinces, reduced to nine in
190 the Hirnantian and only five in the Early to Middle Silurian. In contrast, Rong and Harper
191 (1988) argued only three provinces could be recognized during the Hirnantian, the Edgewood,
192 Kosov (broadly equivalent to the distribution of the typical *Hirnantia* Fauna) and Bani
193 provinces; suggesting this difference in interpretation reflects the relative grouping of
194 increasingly endemic faunas during the glaciation. Brachiopod diversity declines from the
195 tropics into high latitudes (Harper and Mac Niocaill, 2002). In the early part of the Hirnantian
196 the relatively low-diversity *Hirnantia* brachiopod fauna expanded towards the Equator (Temple,
197 1965), replacing the generally more diverse Edgewood Province that dominated the tropics
198 (Harper, 1981; Rong, 1979). A similar pattern is reported with the widely-distributed
199 *Mucronapsis* trilobite fauna (Owen, 1986).

200

201 **Figure 8 about here**

202

203 ***Pattern 4. Benthic extinction was associated with depth.***

204 Detailed analyses indicate the loss in alpha (within community; based on brachiopods) and
205 beta (between community) biodiversity through the extinction events (Brenchley et al., 2001;
206 Fig. 8). During the 1st strike percentage extinctions were high across the shelf but were higher in
207 the outer shelf, Benthic Assemblage 6 (BA 6) characteristic of the outer shelf and upper slope

208 fauna (including the *Foliomena* brachiopod fauna), was completely eradicated. The second
209 strike, further reduced diversity in the mid- and outer shelf biotas (BA 3 and 4/5), including the
210 widespread cool water *Hirnantia* brachiopod fauna (Rong and Harper, 1988).

211 **Geochemical evidence for changing ocean conditions during mass extinction**

212 The Ordovician oceans were very different from those today (e.g., Munnecke et al., 2010).
213 There is no direct evidence for the ventilation of the deep oceans. During the period anoxic
214 ocean bottom waters were widespread and dissolved O₂ concentrations in the mixed layer are
215 hypothesized to have been much reduced compared to the present day (Dahl et al., 2010); though
216 this is difficult to reconcile with the presence of large, complex marine organisms and diverse
217 multi-tiered communities. The fact that a large reservoir of anoxic deep water persisted below
218 the storm and wave influenced mixed layer is corroborated by a number of geochemical and
219 sedimentary proxies. Brenchley and Marshall (1999) argued that the positive $\delta^{13}\text{C}$ isotopic
220 excursion during the Hirnantian, and now reported for earlier events in the Ordovician, could
221 only be realistically sustained with the disposal of ¹²C into anoxic deep oceans though this may
222 be in part due to increased carbonate precipitation rates in eperic seas where high photosynthesis
223 rates in biocalcifying bacteria, maintained by high nutrient fluxes, which locally increased the
224 local carbonate-saturation state of the waters (LaPorte et al., 2009). Geochemical proxies, such
225 as iron speciation, molybdenum concentrations and sulphur isotopes reveal complex patterns of
226 changing regional and global redox conditions through the mass extinction (Figs. 9, 10).

227

228 **Figure 9 about here**

229

230 **Figure 10 about here**

231

232 Sedimentary evidence indicates oxygenated deposition at least at shelfal depths through the
233 peak glaciation (*N. extraordinarius* graptolite biozone), for example there is a widespread shift
234 from deposition of black shale to grey occasionally bioturbated, shale at specific localities (e.g.
235 Dob's Linn; Armstrong and Coe, 1997). This is coincident with pyrite that is significantly
236 enriched in ^{34}S in a number of sections (e.g. Goodfellow and Jonasson, 1984; Hammarlund et al.,
237 2012; Zhang et al., 2009; Fig. 9). The last suggests a widespread reduction in marine sulphate
238 concentrations that can be attributed to an increase in pyrite burial during the early Hirnantian.
239 The ^{34}S -isotope excursion coincides with a major positive carbon isotope excursion recorded
240 globally in marine carbonates (Fig. 9) and indicates increased photic zone photosynthetic
241 productivity and organic carbon flux to the seafloor (Armstrong and Coe, 1997; Bergström et al.,
242 2006; Brenchley et al., 1994; Finney et al., 1999; see also Kump et al., 1999). Together these
243 proxies indicate that as global sea level fell, increased nutrient flux and photic zone bio-
244 productivity intensified, widespread anoxic and in places euxinic conditions prevailed or
245 expanded as the chemocline rose through the water column (Briggs et al., 1988; Fortey, 1989;
246 Goodfellow and Jonasson, 1984; Zhang et al., 2009; though see Hammarlund et al., 2012 for an
247 alternative view).

248 Rapid sea level fall can profoundly affect ocean chemistry, consistent with a pattern of
249 increasing pyrite and organic carbon burial and a rising chemocline. As Hammarland et al
250 (2012) observed as sea level falls, organic carbon produced by primary producers moves farther
251 offshore and sinks through a deeper water column (Wallmann, 2003). The longer settling time of
252 organic carbon leads to a more complete organic carbon decomposition and release and recycling
253 of dissolved inorganic phosphate (DIP). Models show that a sea level drop of 100 m can result in

254 a more than 50% increase in marine DIP concentration, at steady state (Bjerrum et al., 2006;
255 Wallmann, 2003). Consequently more phosphorus becomes available for primary production
256 which in turn feeds back into increased organic matter production, oxygen consumption at depth
257 and carbon burial. During a period of anoxic conditions, enhanced P regeneration from the
258 sediment furthermore creates a positive feedback of P availability (Van Cappellen and Ingall,
259 1997). The last Pleistocene glaciation provides an analogue when deep ocean waters contained
260 less oxygen than during the Holocene (de Boer et al., 2007; Sigman et al., 2004; Toggweiler and
261 Russell, 2008).

262 Associated with these changes at depth an intensification of water column stratification
263 would also steepen the oxygen gradient, reducing the habitable space for the plankton and nekton
264 occupying the dysoxic zone (Berry et al., 1990; Fig. 11).

265 The *N. persculptus* Zone is characterized by a major sea level rise. Redox proxies from a
266 limited number of sections suggest that anoxic, euxinic conditions and even ferruginous waters
267 encroached onto the continental shelves (Hammarlund et al., 2012; Fig. 10). This change
268 coincided with a declining productivity and carbon and pyrite burial, all complexly linked to
269 declining ocean nutrient cycling during the post-glaciation period.

270

271 **TOWARDS A UNIFIED EARTH SYSTEM MECHANISM OF GLACIALLY-INDUCED** 272 **MASS EXTINCTION**

273

274 **Figure 11 about here**

275

276 Figure 11 shows the results of a thought experiment, designed to explain the complex
277 pattern of extinction within the benthos. The model shows the distribution of benthic
278 assemblages from nearshore to offshore. Ecological boundaries within the water column, e.g.
279 fair weather wave base, storm wave base and the chemocline are pinned at the boundaries of the
280 benthic assemblages and maintain their depths during successive phases of the glaciation. This
281 underlying aspect of the model can be tested using paleoecological and sedimentological
282 evidence.

283 Brett et al. (1993) reviewed a variety of sedimentary and fossil evidence that could be used
284 to estimate the absolute depth of the well-established depth gradient of Silurian onshore-to-
285 offshore benthic assemblages (BA 1-5). This constrains much of the spectrum of benthic fossil
286 communities to a narrow depth range, within the photic zone. They placed the depth of Silurian
287 BA 1 through 4 to between 0 and 60 m. The absence of storm-disturbed beds over large parts of
288 several major platforms below about the BA 3-4 boundary constrained the position of storm
289 wave base. This is consistent with reports of Ordovician BA 4 through 6 being found in dysoxic
290 waters below the storm wave base (Potter and Boucot, 1992). A more detailed study of the
291 paleoecological controls of Ordovician benthic assemblages would provide an elegant test of the
292 hypothesis.

293 Figure 11A shows the pre-glaciation template. During the first strike of extinction the
294 expansion of the ice sheet resulted in a ~80m fall in global sea level (Loi et al., 2010) that is
295 coincident with a rise in photosynthetic productivity and the chemocline rose through the water
296 column. The complete extinction of taxa within BA 6 indicates the chemocline rose to shallow
297 continental slope depths. The widths of the BA have been adjusted to maintain the depths of the
298 ecological boundaries as described above. The result is to significantly reduce the widths of the

299 BAs compared to the pre-glaciation mode, particularly in BA 4-5. As shown in Figure 8
300 extinctions during first strike are found in all BAs but are preferentially higher in BA4-6.

301 During the second strike, rapid sea level rise to +100m (Brenchley et al., 1995b; see also
302 Fig. 3) shifts the remaining BAs onshore and coincides with the rise of the chemocline onto the
303 shelf and spread of anoxic/euxinic waters; supported by the redox proxy data. Again the widths
304 of the BAs have been adjusted to maintain the constant depth of the ecological boundaries. The
305 consequence is a further reduction in the widths of BA3 and BA 4-5, but significantly in BA3, a
306 feature associated with higher percentage extinction in this benthic assemblage. The model
307 predicts reduction in prospective niche space at the seafloor is the primary cause of diversity fall.
308 Only BA6 is removed completely and community structures are maintained, though with
309 reduced species richness.

310

311 **DISCUSSION**

312 Species go extinct for two main reasons: 1) population sizes are reduced to a point where
313 chance events result in extinction or, 2) the niches species occupy disappear. Background
314 extinction occurs all the time, but can these mechanisms be extrapolated to explain mass
315 extinctions? At the current resolution of the available datasets it is difficult to test for reduced
316 population sizes. The complex patterns of extinctions during the HME are set against a long
317 term decline in global diversity, from at least the mid-Ordovician. The underlying cause of this
318 decline is currently not understood and may reflect a reduction of ecospace as a response to the
319 gradual cooling prior to the glacial maximum. Alternately, reduction in ecospace may have been
320 provided by the destruction of terranes and microcontinents themselves. Detailed analyses of
321 locality-based databases suggest that the diverse habitats of the island arcs of the Iapetus Ocean

322 were not sustained. This is particularly true for the peri-Laurentian terranes which were accreted
323 to the Laurentian craton during the Appalachian–Caledonian orogeny. Terrane accretion was
324 already underway prior to and during the Hirnantian (Rasmussen and Harper, 2011a).

325 The first strike of the HME has been attributed to cooling, reduced shelf areas as a result of
326 sea-level drop, to globally increased ventilation of the oceans (Berry and Wilde, 1978; Brenchley
327 et al., 1995a), expanding anoxia (Briggs et al., 1988; Fortey, 1989; Goodfellow and Jonasson,
328 1984; Hammarlund et al., 2012; Zhang et al., 2009) and the amalgamation of micro-continents
329 (Rasmussen and Harper, 2011a). For the second strike, anoxia is widely considered the cause as
330 indicated by the widespread deposition of black shale following a rise in sea level (Brenchley et
331 al., 2001; Rasmussen and Harper, 2011a; Rong and Harper, 1988). These hypotheses largely fail
332 to explicitly link the inferred mechanism to the recognized biological explanations for extinction.

333 We hypothesize that coordinated extinctions occurred as a consequence of climatically-
334 induced changes in relative sea level, sea surface temperatures and ocean redox that resulted in
335 the declining availability of prospective niche space in both pelagic/nektonic and benthic species
336 (Fig. 12).

337

338 **Figure 12 about here**

339

340 This is a modification of the “shelf area hypothesis” which posits a relationship between
341 species richness and habitable area, Phanerozoic species richness appears to have been in
342 equilibrium with habitable area (Sepkoski, 1976). In the latest manifestation of this hypothesis
343 Finnegan et al (2012) reported, based on sections from Laurentia, a link between tropical cooling
344 and habitat loss. Sclafani and Holland (2013) also showed, using census data from Upper

345 Ordovician strata in Laurentia, a weak positive relationship between province area defined on
346 geochemical parameters, and biodiversity though this was based on an untested assumption that
347 Early Paleozoic communities were species saturated.

348 During the first phase of the HME, major eustatic sea-level fall removed significant
349 habitable area on the continental shelves which lead to the down-shelf displacement of benthic
350 assemblages, that coincided with a rise in the chemocline and an increase oxygen gradient
351 reducing the habitable space for the plankton and nekton occupying the dysoxic zone in the
352 oceans. Within the mixed layer declining diversity in planktonic provinces during the glacial
353 maximum resulted from the steepening of latitudinal temperature gradients; which in turn
354 resulted in the equator-ward spread of the low diversity Polar Province and the narrowing of high
355 diversity provinces in the mid- latitudes.

356 During the eustatic sea level rise in the *persculptus* graptolite biozone, the potential
357 increase of habitable shelf area was balanced by a narrowing of the shelf area occupied by BA 3
358 through 4/5 as ferruginous/euxinic water masses encroached onto the outer shelves, to close to
359 storm wave base. During this interval the rise of the chemocline onto the shelves reduced
360 habitable space coincident with a decline in diversity (Brenchley et al., 2001). The long-term
361 ventilation of the oceans (Saltzman, 2005) and the deepening of the chemocline broke the link
362 between glaciation and mass extinction.

363 A reduction in the area/volume occupied by a community either at the seafloor, within the
364 water column or at the sea surface increased competition and selection pressures leading to
365 extinctions where the carrying capacities of particular ecological niches were exceeded (Harper
366 et al., 2013 in press; Saltzman, 2005; Sheehan, 1975, 2008; Valentine, 1969). In this way, within
367 community extinctions are the predicted pattern of diversity change during the HME.

368 The availability of prospective niche space has implications not only for elevated
369 extinction but post-extinction recovery. In the allopatric model of speciation, incipient new
370 species arise continually as a consequence of gene mutation and allopatry. The constraint on the
371 fixing of new species is the availability of expanding ecospace (Erwin, 2001). In this model
372 recovery from the HME could not be initiated until ocean stratification and chemistry had
373 returned to the pre-glacial equilibrium state..

374

375 **CONCLUSIONS**

- 376 • The HME coincided with the glacial maximum of the Early Palaeozoic Icehouse.
- 377 • Existing causative hypotheses fail to provide a biological context for the HME .
- 378 • We hypothesize that coordinated extinctions occurred as a consequence of glacially-
379 induced changes in sea surface temperatures and ocean oxygen stratification that resulted
380 in the declining availability of prospective niche space in both pelagic and benthic realms.
- 381 • During the first phase of the HME, major eustatic sea-level fall coincident with a rise in the
382 chemocline and a steepening of the water column oxygen gradient, displaced benthic
383 communities offshore into reduced habitable areas. Declining diversity in the plankton
384 resulted from the steepening of latitudinal temperature gradients; resulting in the equator-
385 ward spread of the low diversity Polar Province and the narrowing of high diversity
386 provinces in the mid- latitudes.
- 387 • Following glacial termination, eustatic sea level rise in the *persculptus* graptolite biozone,
388 a potential increase of habitable shelf area was balanced by a narrowing of the shelf area
389 occupied by BA 3 through 4/5 as ferruginous/euxinic water masses encroached onto the
390 outer shelves, to close to storm wave base.

- 391 • Together each phase of mass extinction can be related to a loss of habitable area and a
392 reduction in prospective niche space. Elevated density dependent competition resulted in
393 high levels of within community species extinction.
- 394 • HME was contingent on the unique nature of the Early Paleozoic oceans, with deep ocean
395 anoxia. The effects of glaciations during the earlier Ordovician have yet to be studied in
396 detail.
- 397 • The progressive ventilation of the oceans during the later Paleozoic and Mesozoic meant
398 the biosphere would never again be subject to glacially-induced mass extinction.

399 **ACKNOWLEDGMENTS**

400 We thank the conference conveners who have provided an opportunity to present and discuss our
401 ideas. The Mineralogical Society provided financial support. DATH is funded by Danish
402 Council for Independent Research. We acknowledge the comments of our referees Prof. M.
403 Williams and Dr A. W. Owen and the editor whose work greatly improved the manuscript.

404

405 **REFERENCES CITED**

- 406 Adrain, J., Edgecombe, G. D., Fortey, R. A., Hammer, Ø., Laurie, J. R., McCormick, T., Owen,
407 A. W., Waisfeld, B. G., Webby, B. D., Westrop, S. R., and Zhou, Z.-y., 2004, Trilobites,
408 *in* Webby, B. D., Paris, F., Droser, M. L., and Percival, I. G., eds., The Great Ordovician
409 Biodiversification Event: New York, Columbia University Press, p. 231-254.
- 410 Armstrong, H. A., 2007, On the cause of the Ordovician glaciation, in Williams, M., Haywood,
411 A., and Gregory, J., eds., Deep time perspectives on climate change, Volume Special
412 Publication of the Geological Society of London: London, The Micropalaeontological
413 Society and Geological Society of London, p. 101-121.

414 Armstrong, H. A., and Coe, A. L., 1997, Deep sea sediments record the geophysiology of the end
415 Ordovician glaciation.: *Journal of the Geological Society*, v. 154, p. 929-934.

416 Baarlie, B. G., and Harper, D. A. T., 1986, Relict Ordovician brachiopod faunas in the Lower
417 Silurian of Asker, Oslo Region, Norway: *Norsk Geologiske Tidsskrift*, v. 66, p. 87-91.

418 Bambach, R. K., Knoll, A. H., and Wang, S., 2004, Origination, extinction, and mass depletions
419 of marine diversity: *Paleobiology*, v. 30, no. 4, p. 522-542.

420 Bapst, D. W., Bullock, P. C., Melchin, M. J., Sheets, H. D., and Mitchell, C. E., 2012, Graptoloid
421 diversity and disparity became decoupled during the Ordovician mass extinction:
422 *Proceedings of the National Academy of Sciences*, v. 109, p. 3428-3433.

423 Bergström, S. M., Chen, X. U., Gutiérrez-Marco, J. C., and Dronov, A., 2009, The new
424 chronostratigraphic classification of the Ordovician System and its relations to major
425 regional series and stages and to $\delta^{13}\text{C}$ chemostratigraphy: *Lethaia*, v. 42, no. 1, p. 97-107.

426 Bergström, S. M., Saltzman, M. R., and Schmitz, B., 2006, First record of the Hirnantian (Upper
427 Ordovician) delta C-13 excursion in the North American Midcontinent and its regional
428 implications.: *geological Magazine*, v. 143, p. 657-678.

429 Berry, W. B. N., and Wilde, P., 1978, Progressive ventilation of the oceans-an explanation for
430 the distribution of the Lower Paleozoic black shales: *American Journal of Science*, v.
431 278, p. 27-75.

432 Berry, W. B. N., Wilde, P., and Quinby-Hunt, M., 1990, Late Ordovician Graptolite Mass
433 Mortality and Subsequent early Silurian Re-radiation, *Extinction Events in Earth History:*
434 *Lecture Notes in Earth Sciences Volume 30: Berlin, Springer Verlag.*

435 Bjerrum, C. J., Bendtsen, J., and Legarth, J. J. F., 2006, Modeling organic carbon burial during
436 sea level rise with reference to the Cretaceous 1–24.: *Geochemistry Geophysics*
437 *Geosystems*, v. 7, p. 1-24.

438 Boulila, S., Galbrun, B., Miller, K. G., Pekar, S. F., Browning, J. V., Laskar, J., and Wright, J.
439 D., 2011, On the origin of Cenozoic and Mesozoic "third-order" eustatic sequences:
440 *Earth-Science Reviews*, v. 109, p. 94-112.

441 Brenchley, P. J., Carden, G. A. F., and Marshall, J. D., 1995a, Environmental changes associated
442 with the 'first strike' of the Late Ordovician mass extinction: *Modern Geology*, v. 20, p.
443 69-82.

444 Brenchley, P. J., and Cullen, B., 1984, The environmental distribution of associations belonging
445 to the Hirnantia fauna-evidence from North Wales and Norway, in Bruton, D. L., ed.,
446 *Aspects of the Ordovician System*, Volume 295.

447 Brenchley, P. J., and Marshall, J. D., 1999, Relative timing of critical events during the late
448 Ordovician mass extinction-new data from Oslo: *Acta Universitatis Carolinae*,
449 *Geologica*, v. 43, p. 187-191.

450 Brenchley, P. J., Marshall, J. D., Carden, G. A. F., Robertson, D. B. R., Long, D. G., Meidla, T.,
451 Hints, L., and Anderson, T. F., 1994, Bathymetric and isotopic evidence for a short lived
452 Late Ordovician glaciation in a greenhouse period: *Geology*, v. 22, p. 295-298.

453 Brenchley, P. J., Marshall, J. D., Carden, G. A. F., Robertson, D. B. R., Long, D. G., Meidla, T.,
454 Hints, L., and Anderson, T. F., 1995b, Bathymetric and isotopic evidence for a short-
455 lived late Ordovician glaciation in a greenhouse period.: *Geology*, v. 22, p. 295-298.

456 Brenchley, P. J., Marshall, J. D., Harper, D. A. T., Buttler, C. J., and Underwood, C. J., 2006, A
457 late Ordovician (Hirnantian) karstic surface in a submarine channel, recording

458 glacioeustatic sea-level changes: Meifod, central Wales. : Geological Journal v. 41, p. 1-
459 22.

460 Brenchley, P. J., Marshall, J. D., and Underwood, C. J., 2001, Do all mass extinctions represent
461 an ecological crisis? Evidence from the Late Ordovician: Geological Journal, v. 36, no.
462 329-340.

463 Brett, C. E., Boucot, A. J., and Jones, B., 1993, Absolute depths of Silurian benthic assemblages:
464 Lethaia, v. 26, no. 1, p. 25-40.

465 Brett, C. E., Hendy, A. J. W., Bartholomew, A. J., Bonelli, J. R., and McLaughlin, P. I., 2007,
466 Response of shallow marine biotas to sea-level fluctuations: a review of faunal
467 replacement and the process of habitat tracking.: Palaios, v. 22, no. 3, p. 228-244.

468 Briggs, D. E. G., Fortey, R. A., and Clarkson, E. N. K., 1988, Extinction and the fossil record of
469 the arthropods, in Larwood, G., ed., Systematics Association Special Volume 34: Oxford,
470 Clarendon Press, p. 171-209.

471 Copper, P., and Jin, J., 2012, Early Silurian (Aeronian) East Point coral patch reefs of Anticosti
472 Island, Eastern Canada: first reef recovery from the Ordovician/Silurian Mass Extinction
473 in Eastern Laurentia: Geosciences, v. 2, p. 64-89.

474 Cooper, R. A., Fortey, R. A., and Lindholm, K., 1991, Latitudinal and depth zonation of early
475 Ordovician graptolites: Lethaia, v. 24, no. 2, p. 199-218.

476 Dahl, T. W., Hammarlund, E. U., Anbar, A. D., Bond, D. P. G., Gill, B. C., Gordon, G. W.,
477 Knoll, A. H., Nielsen, A. T., Schovsbo, N. H., and Canfield, D. E., 2010, Devonian rise
478 in atmospheric oxygen correlated to the radiations of terrestrial plants and large predatory
479 fish: Proceedings of the National Academy of Sciences v. 107, p. 17911-17915.

480 de Boer, A. M., Sigman, D. M., Toggweiler, J. R., and Russell, J. L., 2007, Effect of global
481 ocean temperature change on deep ocean ventilation: *Paleoceanography*, v. 22.

482 Droser, M. L., Bottjer, D. J., and Sheehan, P. M., 1997, Evaluating the ecological architecture of
483 major events in the Phanerozoic history of marine invertebrate life: *Geology*, v. 25, p.
484 167-170.

485 Droser, M. L., Bottjer, D. J., Sheehan, P. M., and McGhee, G. R., 2000, Decoupling of
486 taxonomic and ecologic severity of Phanerozoic marine mass extinctions: *Geology*, v. 28,
487 no. 8, p. 675-678.

488 Erwin, D. H., 2001, Lessons from the past: evolutionary impacts of mass extinctions.:
489 *Proceedings National Academy of Sciences, USA*, v. 98, p. 5399-5403.

490 Finnegan, S., Heim, N. A., Peters, S. E., and Fischer, W. W., 2012, Climate change and the
491 selective signature of the Late Ordovician mass extinction: *Proceedings of the National*
492 *Academy of Sciences*, v. 109, no. 18, p. 6829-6834.

493 Finnegan, S., Bergmann, K., Eiler, J. M., Jones, D. S., Fike, D. A., Eisenman, L., Hughes, N. C.,
494 Tipati, A. K., and Fischer, W. W., 2011, The magnitude and duration of the Late
495 Ordovician-Early Silurian glaciation: *Science*, v. 331, p. 903-906.

496 Finney, S. C., and Berry, W. B. N., 1997, New perspectives on graptolite distributions and their
497 use as indicators of platform margin dynamics: *Geology*, v. 25, no. **10**, p. 919-922.

498 Finney, S. C., Berry, W. B. N., Cooper, J. D., Ripperdan, R. L., Sweet, W. C., Jacobson, S. R.,
499 Soufiane, A., Achab, A., and Noble, P. J., 1999, Late Ordovician mass extinction: a new
500 perspective from stratigraphic sections in central Nevada: *Geology* v. 27, p. 215-218.

501 Fortey, R. A., 1989, There are extinctions and extinctions - examples from the Lower
502 Palaeozoic: Philosophical Transactions of the Royal Society of London - Series B:
503 Biological Sciences, v. 325, p. 327-355.

504 Fortey, R. A., Harper, D. A. T., Ingham, J. K., Owen, A. W., and Rushton, A. W. A., 1995, A
505 revision of Ordovician series and stages from the historical type area: Geological
506 Magazine, v. 132, p. 15-30.

507 Godderis, Y., Francois, L. M., and Veizer, J., 2001, The early Paleozoic carbon cycle: Earth and
508 Planetary Science Letters, v. 190, p. 181-196.

509 Goodfellow, W. D., and Jonasson, I. R., 1984, Ocean stagnation and ventilation defined by $\delta^{34}\text{S}$
510 secular trends in pyrite and barite, Selwyn Basin, Yukon: Geology, v. 112, p. 583-586.

511 Hammarlund, E. U., Dahl, T. W., Harper, D. A. T., Bond, D. P. G., Nielsen, A. T., Bjerrum, C.
512 J., Schovsbo, N. H., Schonlaub, H. P., Zalasiewicz, J. A., and Canfield, D. E., 2012, A
513 sulfidic driver for the end-Ordovician mass extinction: Earth and Planetary Science
514 Letters, v. 331-332, p. 128-139.

515 Haq, B. U., and Schuller, S. R., 2008, A chronology of Paleozoic sea-level changes: Science, v.
516 322, p. 64-68.

517 Harper, D. A. T., 1981, The stratigraphy and faunas of the Upper Ordovician High Mains
518 Formation of the Girvan district. : Scottish Journal of Geology v. 17, p. 247-255.

519 Harper, D. A., and MacNiocaill, C., 2002, Early Ordovician rhynchonelliformean brachiopod
520 biodiversity: comparing some platforms, margins and intra-oceanic sites around the
521 Iapetus Ocean: Geological Society, London, Special Publications, v. 194, no. 1, p. 25-34.

522 Harper, D. A. T., Hammarlund, E. U., and Rasmussen, C. M. Ø., 2013 (in press), End
523 Ordovician extinctions: A coincidence of causes: Gondwana Research.

524 Harper, D. A. T., and Rong, J., 2008, Completeness of the Hirnantian brachiopod record: spatial
525 heterogeneity through the end Ordovician extinction event: *Lethaia* v. 41, p. 195-197.

526 Holmden, C., Panchuk, K., and Finney, S. C., 2012, Tightly coupled records of Ca and C isotope
527 changes during the Hirnantian glaciation event in an epeiric sea setting: *Geochimica et*
528 *Cosmochimica Acta*, v. 98, p. 94-106.

529 Jablonski, D., 1991, Extinctions: a paleontological perspective: *Science*, v. 253, p. 754-757.

530 Kucera, M., 2007, Planktonic foraminifera as traces of past oceanic environments in proxies in
531 late Cenozoic palaeoceanography, in C Hillaire-Marce, C., and De Vernal, A., eds.,
532 *Developments in Marine Geology, Volume 1: Amsterdam, Elsevier*, p. 213-262.

533 Kump, L. R., Arthur, M. A., Patzkowsky, M. E., Gibbs, M. T., Pinkus, D. S., and Sheehan, P.
534 M., 1999, A weathering hypothesis for glaciation at high atmospheric pCO₂ during the
535 Late Ordovician.: *Palaeogeography Palaeoclimatology Palaeoecology*, no. 152, p. 173-
536 187.

537 LaPorte, D. F., Holmden, C., Patterson, W. P., Loxton, J. D., Melchin, M. J., Mitchell, C. E.,
538 Finney, S. C., and Sheets, H. D., 2009, Local and global perspectives on carbon and
539 nitrogen cycling during the Hirnantian glaciation: *Palaeogeography, Palaeoclimatology,*
540 *Palaeoecology*, v. 276, p. 182-195.

541 Loi, A., Ghienne, J. F., Dabard, M. P., Paris, F., Botquelen, A., Christ, N., Elaouad-Debbaj, Z.,
542 Gorini, A., Vidal, M., Videt, B., and Destombes, J., 2010, The Late Ordovician glacio-
543 eustatic record from a high-latitude storm-dominated shelf succession: The Bou Ingarf
544 section (Anti-Atlas, Southern Morocco): *Palaeogeography, Palaeoclimatology,*
545 *Palaeoecology*, v. 296, no. 3-4, p. 332-358.

546 McGhee Jr, G. R., Clapham, M. E., Sheehan, P. M., Bottjer, D. J., and Droser, M. L., 2013, A
547 new ecological-severity ranking of major Phanerozoic biodiversity crises:
548 *Palaeogeography, Palaeoclimatology, Palaeoecology*, v. 370, no. 0, p. 260-270.

549 Munnecke, A., Calner, M., Harper, D. A. T., and Servais, T., 2010, Ordovician and Silurian
550 seawater chemistry and climate: A synopsis: *Palaeogeography, Palaeoclimatology,*
551 *Palaeoecology*, v. 296, p. 389-413.

552 Nardin, E., Godd ris, Y., Donnadieu, Y., Hir, G. L., Blakey, R. C., Puc at, E., and Aretz, M.,
553 2011, Modeling the early Paleozoic long-term climatic trend: *Geological Society of*
554 *America Bulletin*, v. 123, no. 5-6, p. 1181-1192.

555 Owen, A. W., 1986, The uppermost Ordovician (Hirnantian) trilobites of Girvan, SW Scotland
556 with a review of coeval trilobite faunas: *Transactions of the Royal Society of Edinburgh:*
557 *Earth Sciences*, v. 77, p. 231-239.

558 Owen, A. W., Harper, D. A. T., and Heath, R. A., 2008, A route to recovery: The early Silurian
559 shallow-water shelly fauna in the northern Oslo basin: *Lethaia*, v. 41, no. 2, p. 173-184.

560 Potter, A. W., and Boucot, A. J., 1992, Middle and Late Ordovician brachiopod benthic
561 assemblages of North America, Rotterdam, Balkema, *Global Perspectives on Ordovician*
562 *Geology*, 307-323 p.:

563 Rasmussen, C. M.  ., and Harper, D. A. T., 2011a, Did the amalgamation of continents drive
564 the end Ordovician mass extinctions?: *Palaeogeography, Palaeoclimatology,*
565 *Palaeoecology*, v. 311, p. 48-62.

566 -, 2011b, Interrogation of distributional data for the end-Ordovician crisis interval: where did the
567 disaster strike?: *Geological Journal*, v. 46, p. 478-500.

568 Rong, J., 1979, The Hirnantia fauna of China with comments on the Ordovician–Silurian
569 boundary. (In Chinese). *Journal of Stratigraphy* v. 3, p. 1-29

570 Rong, J., and Harper, D. A. T., 1988, A global synthesis of the latest Ordovician Hirnantian
571 brachiopod faunas: *Transactions Royal Society of Edinburgh: Earth Sciences*, v. 79, p.
572 383-402.

573 -, 1999, Brachiopod survival and recovery from the latest Ordovician mass extinctions in South
574 China: *Geological Journal*, v. 34, no. 4, p. 321-348.

575 Rong, J.-Y., and Zhan, R.-B., 2006, Surviving the end-Ordovician extinctions: evidence from the
576 earliest Silurian brachiopods of northeastern Jiangxi and western Zhejiang provinces,
577 East China: *Lethaia*, v. 39, no. 1, p. 39-48.

578 Rong, J.-Y., Boucot, A. J., Harper, D. A. T., Zhan, R., and Neuman, R. B., 2006, Global analyses
579 of brachiopods faunas through the Ordovician and Silurian transition: reducing the role of
580 the Lazarus effect.: *Canadian Journal of Earth Sciences*, v. 43, p. 23-39.

581 Saltzman, M. R., 2005, Phosphorus, nitrogen and the redox evolution of the Paleozoic oceans.:
582 *Geology*, v. 33, p. 573-576.

583 Sclafani, J. A., and Holland, S. M., 2013, The Species-Area Relationship in the Late Ordovician:
584 A Test Using Neutral Theory: *Diversity*, v. 5, p. 240-262.

585 Sepkoski, J. J., Jr., 1976, Species Diversity in the Phanerozoic: Species-Area Effects:
586 *Paleobiology*, v. 2, no. 4, p. 298-303.

587 -, 1981, A factor analytic description of the marine fossil record: *Paleobiology*, v. 7, no. 36-53.

588 -, 1995, The Ordovician radiations: diversification and extinction shown by the global genus-
589 level taxonomic data, in Cooper, J. D., Droser, M. L., and Finney, S. C., eds., *Ordovician*
590 *Odyssey: Short Papers for the Second International Symposium on the Ordovician*

591 System: Fullerton, California, Pacific Section, Society for Economic Paleontologists and
592 Mineralogists, p. 393-396.

593 Sepkoski Jr, J. J., 1996, Patterns of Phanerozoic extinction: a perspective from global databases.,
594 *in* Walliser, O. H., ed., *Global Events and Event Stratigraphy in the Phanerozoic*: Berlin,
595 Springer, p. 35-51.

596 Servais, T., Lehnert, O., Li, J., Miullins, G. L., Munnecke, A., Nutzel, A., and Vecoli, M., 2008,
597 *The Ordovician Biodiversification: revolution in the oceanic trophic chain.:* *Lethaia*, v.
598 41, p. 99-109.

599 Sheehan, P. M., 1975, Brachiopod synecology in a time of crisis (Late Ordovician–Early
600 Silurian): *Paleobiology*, v. 1, p. 205-212.

601 -, 2008, Did incumbency play a role in maintaining boundaries between Late Ordovician
602 brachiopod realms?: *Lethaia*, v. 41, p. 147-153.

603 Sheehan, P. M., and Coorough, P. J., 1990, Brachiopod zoogeography across the Ordovician-
604 Silurian extinction event: *Geological Society, London, Memoirs*, v. 12, p. 181-187.

605 Sigman, D. M., Jaccard, S. L., and Haug, G. H., 2004, Polar ocean stratification in a cold
606 climate: *Nature*, v. 428, p. 59-63.

607 Temple, J. T., 1965 Upper Ordovician brachiopods from Poland and Britain.: *Acta*
608 *Palaeontologica Polonica*, v. 10, p. 379-427.

609 Toggweiler, J. R., and Russell, J., 2008, Ocean circulation in a warming climate: *Nature*, v. 451,
610 p. 286-288.

611 Trotter, J. A., Williams, I. S., Barnes, C. R., Lecuyer, C., and Nicoll, R. S., 2008, Did cooling
612 oceans trigger Ordovician biodiversification? Evidence from conodont thermometry:
613 *Science*, v. 321, p. 550-554.

614 Turner, B. R., Armstrong, H. A., and Holt, P., 2011, Visions of ice sheets in the Early
615 Ordovician greenhouse world: Evidence from the Peninsula Formation, Cape Peninsula,
616 South Africa: *Sedimentary Geology*, v. 236, p. 226-238.

617 Turner, B. R., Armstrong, H. A., Wilson, C. R., and Makhlof, I. M., 2012, High frequency
618 eustatic sea-level changes during the Middle to early Late Ordovician of southern Jordan:
619 Indirect evidence for a Darriwilian Ice Age in Gondwana: *Sedimentary Geology*, v. 251-
620 252, p. 34-48.

621 Underwood, C. J., Crowley, S. F., Marshall, J. D., and Brenchley, P. J., 1997, High resolution
622 carbon isotope stratigraphy of the basal Silurian stratotype (Dob's Linn, Scotland) and its
623 global correlation.: *Journal of the Geological Society, London*, v. 154, p. 709-718.

624 Valentine, J. W., 1969, Patterns of taxonomic and ecological structure of the shelf benthos
625 during Phanerozoic time: *Palaeontology*, v. 12, p. 684-709.

626 Valentine, J. W., and Jablonski, D., 1991, Biotic effects of sea level change: The Pleistocene test:
627 *Journal of Geophysical Research: Solid Earth*, v. 96, no. B4, p. 6873-6878.

628 Van Cappellen, P., and Ingall, E. D., 1997, Redox stabilization of the atmosphere and oceans and
629 marine productivity: *Science*, v. 275, p. 406-408.

630 Vandembroucke, T. R. A., Armstrong, H. A., Williams, M., Paris, F., Sabbe, K., Zalasiewicz, J.
631 A., Nölvak, J., and Verniers, J., 2010a, Epipelagic chitinozoan biotopes map a steep
632 latitudinal temperature gradient for earliest Late Ordovician seas: Implications for a
633 cooling Late Ordovician climate: *Palaeogeography, Palaeoclimatology, Palaeoecology*, v.
634 294, no. 3-4, p. 202-219.

635 Vandembroucke, T. R. A., Armstrong, H. A., Williams, M., Paris, F., Zalasiewicz, J. A., Sabbe,
636 K., Nölvak, J., Challands, T. J., Verniers, J., and Servais, T., 2010b, Polar front shift and

637 atmospheric CO₂ during the glacial maximum of the Early Paleozoic Icehouse:
638 Proceedings of the National Academy of Sciences, v. 107, no. 34, p. 14983-14986.
639 Vandembroucke, T. R. A., Armstrong, H. A., Williams, M., Zalasiewicz, J. A., and Sabbe, K.,
640 2009, Ground-truthing Late Ordovician climate models using the palaeobiology of
641 graptolites: : Palaeoceanography, v. 24, p. PA4202.
642 Wallmann, K., 2003, Feedbacks between oceanic redox states and marine productivity: a model
643 perspective focused on benthic phosphorus cycling: Global Biogeochemical Cycles, v.
644 17.
645 Webby, B. D., Paris, F., Droser, M. L., and Percival, I. G., 2004, The Great Ordovician
646 Biodiversification Event., New York, Columbia University Press.
647 Yan, D., Chen, D., Wang, Q., and Wang, J., 2009, Geochemical changes across the Ordovician-
648 Silurian transition on the Yangtze Platform, South China: Science in China Series D:
649 Earth Sciences, v. 52, no. 1, p. 38-54.
650 Zalasiewicz, J. A., Taylor, L., Rushton, A. W. A., Loydell, D. K., Rickards, R. B., and Williams,
651 M., 2009, Graptolites in British stratigraphy: Geological Magazine, v. 146, p. 785-850.
652
653 Zhang, T. G., Shen, Y. N., Zhan, R. B., Shen, S. Z., and Chen, X., 2009, Large perturbations of
654 the carbon and sulfur cycle associated with the Late Ordovician mass extinction in South
655 China: Geology v. 37, p. 299-302.

656
657 **FIGURE CAPTIONS**

658 Figure 1. Global biodiversity changes through the Phanerozoic. Family diversity of marine
659 animals through the Phanerozoic indicating the three evolutionary faunas and microfossil record.
660 The major extinction events (end Ordovician, late Devonian, end Permian, end Triassic and end

661 Cretaceous) are shown (after Sepkoski (1981)). Solid arrows indicate mass extinctions where
662 extinction rates exceed small increases in originations; dashed arrows indicate mass extinctions
663 where reductions in origination exceed extinction.

664

665 Figure 2. Biotic change through the Hirnantian mass extinction. The brachiopod data indicate
666 the generic loss that appears to have been initiated already within the *pacificus* graptolite
667 biozone. After Brenchley et al., 2001 with modified brachiopod data from Rasmussen and
668 Harper, 2011b).

669

670 Figure 3. Late Ordovician-Early Silurian stratigraphy, stable isotope stratigraphy and relative sea
671 level change. The base of the Hirnantian is placed at the base of the *extraordinarius* graptolite
672 biozone after Underwood et al., 1997). The carbon isotope profile is modified from Brenchley et
673 al., 1994 and the sea level curve is from Brenchley et al., 1995b). (Figure modified from
674 Brenchley et al., 2001).

675

676 Figure 4. Modelled atmospheric carbon dioxide and tropical sea surface temperatures through the
677 Cambrian to Silurian. Tropical sea surface temperatures are from Nardin et al. (2011), with the
678 grey area indicating the error envelope. Atmospheric carbon dioxide after Godderis et al., 2001).

679

680 Figure 5. Time stratigraphical diagram showing the chronostratigraphy and global composite
681 proxy data. (A, B) Data for relative sea level (after Haq and Schulte, 2008). (C) Stable carbon
682 (after Bergström et al., 2009). Grey horizontal boxes in B highlight the time periods of ~1.2 myr
683 cyclic changes in global sea level, interpreted as indicative of icehouse periods. GCIE is the

684 Guttenburg Carbon Isotope Excursion, HCIE is the Hirnantian Carbon Isotope Excursion. (After
685 Turner et al., 2011).

686

687 Figure 6. Biotic diversity during the Cambrian to Silurian. A. Benthic generic diversity. B.
688 Pelagic and nektonic taxonomic diversity. (Data from Sepkoski Online, downloaded March
689 2013). Note the data are assembled in the database using the British Series names. The Llanvirn
690 was extended by Fortey et al. (1995) to include part of the classical Llandeilo Series as a stage.
691 For convenience these are retained where appropriate in the text. British and globally recognised
692 divisions are compared in Figure 5.

693

694 Figure 7. Late Ordovician Polar Front migration. The figure compares the spatial distribution of
695 Sandbian, Hirnantian chitinozoan and graptolites and modern planktonic foraminiferan
696 provinces. The changing position of graptolite and chitinozoan provinces show an equator-ward
697 shift in the position of the Polar Front from 55° to 70° S to likely 40° S. This involves an
698 equator-ward incursion of Polar water and a narrowing of the Subpolar Province. The
699 Subtropical province moves slightly northwards. The migration of the Hirnantian Polar Front
700 compares well with known patterns from late Cenozoic interglacial to glacial transitions. (After
701 Vandenbroucke et al., 2010b).

702

703 Figure 8. Changes within brachiopod community (alpha) diversity across the continental shelf
704 and upper slope as calculated by Brenchley et al (2001). Numbers are an average taken from
705 communities within the benthic assemblage zones. There are no data for benthic assemblage 1.
706 Numbers in bold indicate the percentage decrease in mean alpha diversity at the first and second

707 strikes. The fall in alpha diversity after the first phase of extinction also includes the addition of
708 new taxa belonging to the Hirnantian recovery fauna; no similar recovery fauna buffers the effect
709 of the second phase of extinction. (Modified from Brenchley et al., 2001).

710

711 Figure 9. The Hirnantian mass extinction, glaciation and isotope excursions (from Hammarlund
712 et al., 2012). A) Four major marine groups affected by the two-phased end Ordovician
713 extinction, pre-, Hirnantian and post-Hirnantian refer to faunas (Brenchley et al., 1994). B)
714 Interpolated $\delta^{18}\text{O}$ reflect fluctuations of Rawtheyan and Hirnantian sea level (Finnegan et al.,
715 2011); LGM is the Last Glacial Maximum. C) Equatorial temperature fluctuations broadly
716 parallel the $\delta^{18}\text{O}$ curve (Finnegan et al., 2011). D) A compilation of three profiles of inorganic
717 $\delta^{13}\text{C}$ shows a significant perturbation of oceanic carbon cycle dynamics during the Hirnantian
718 (Kump et al., 1999; LaPorte et al., 2009). E) A compilation of sulphur isotope data shows a
719 major perturbation during the Hirnantian that parallels the $\delta^{13}\text{C}$ curve (Yan et al., 2009;
720 Hammarlund et al., 2012).

721

722 Figure 10. Iron and molybdenum data for the sections at Dob's Linn, Scotland (GSSP for the
723 base of the Silurian) and Billegrav, Denmark, reveal extensive euxinic, and occasional
724 ferruginous, conditions. FeHR/FeT, highly reactive iron over total iron, has a threshold at 0.38.
725 FePY/FeHR, the ratio of pyrite over highly reactive iron, filled circles are values above and open
726 circles below 0.7. Mo, concentrations (ppm). The grey zone indicates the interval which is
727 discussed as a lowermost threshold for euxinic conditions. (After Hammarlund et al., 2012).

728

729 Figure 11. Conceptual model illustrating the paleoenvironmental changes associated with
730 evolving sea level changes (rsl). Stars indicate the areas with greatest biodiversity decline. Fair
731 weather wave base (fwwb), storm wave base (swb) and pycnocline are fixed at the benthic
732 assemblage boundaries and maintain their depths during sea level change. The consequence is to
733 change the habitable area occupied by the benthic assemblages. Changes in habitable area are
734 consistent with areas of maximum species loss as shown in Figure 8.

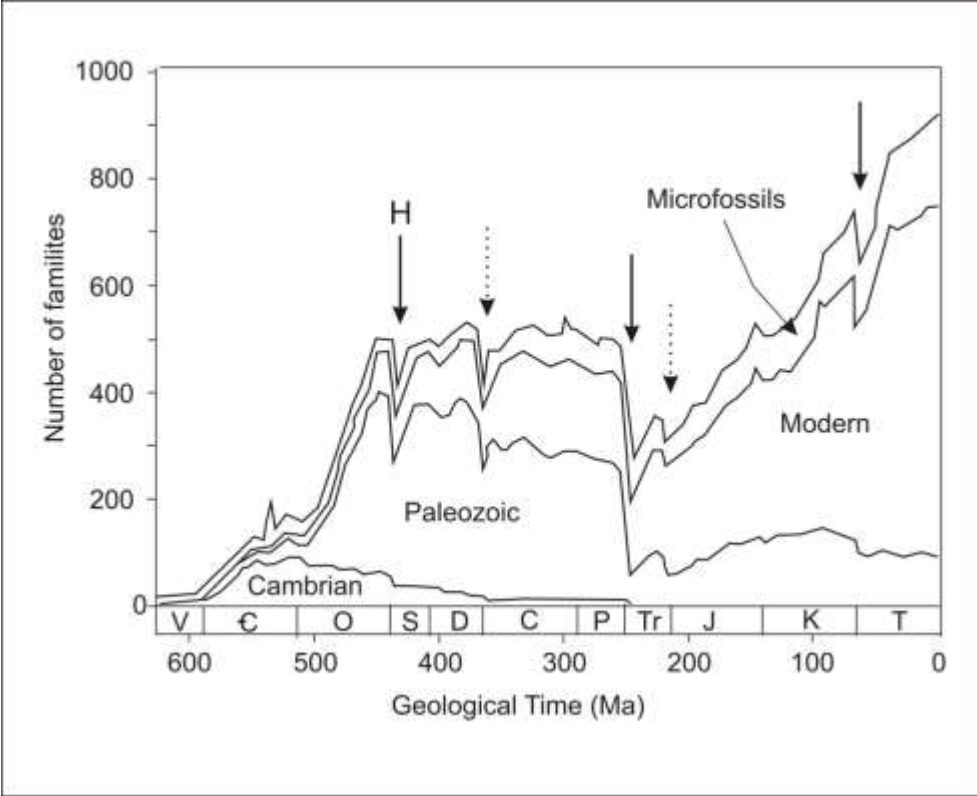
735

736 Figure 12. Model showing the combined effects of oceanographical and climatic changes during
737 the mass extinction. Changing latitudinal temperature gradients affect the width and distribution
738 of the planktonic provinces (Polar, Subpolar, Tr, Transitional, Subtropical-Tropical).

739 Simultaneously, oceanographical changes associated with changing sea level and ocean redox
740 gradients affected benthic communities (f, fair weather wave base; s, storm wave base; c,
741 chemocline). The chemocline marks the top of anoxic deep ocean water. The combined effects
742 of both these processes was to reduce the habitable areas/prospective niche space and hence
743 increase competition between species leading to extinctions where the carrying capacities of
744 particular ecological niches were exceeded. Note there is are no continents on the North Pole to
745 support a major ice sheet.

746

747



748

749 Figure 1

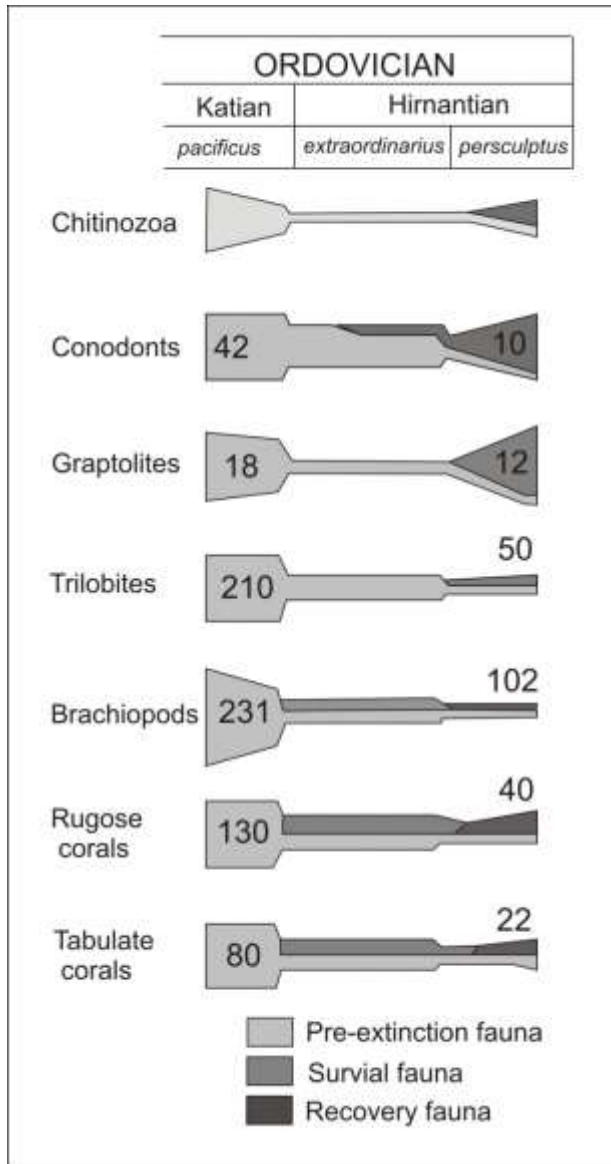
750

751

752 Figure 2

753

754

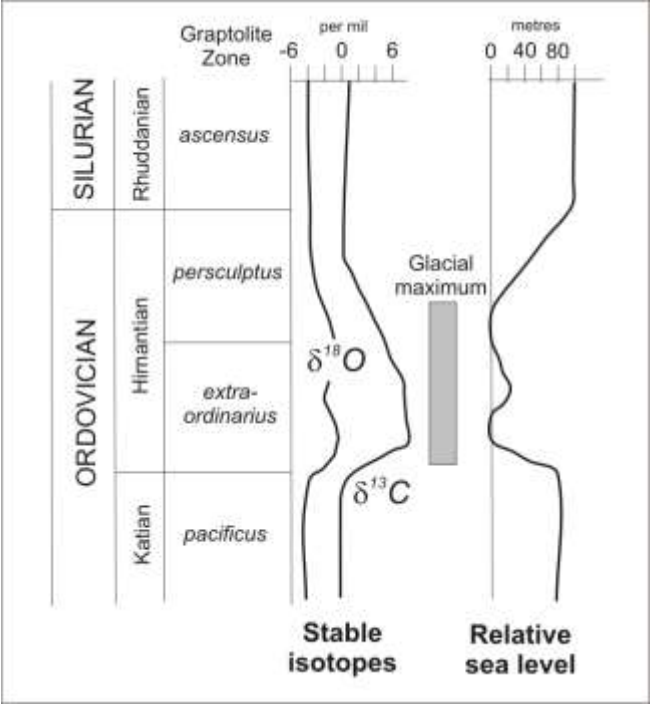


755

756

757

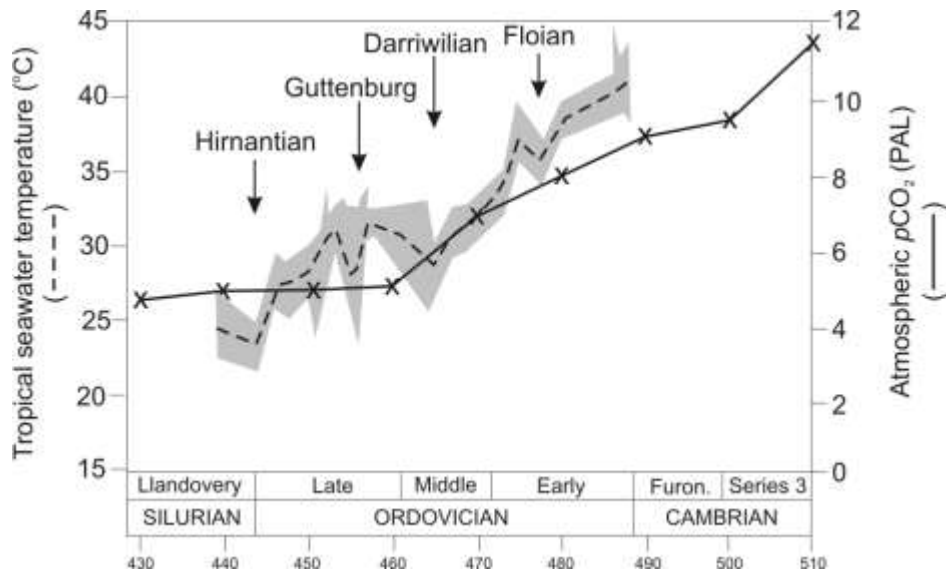
758 Figure 3



759

760

761 Figure 4



762

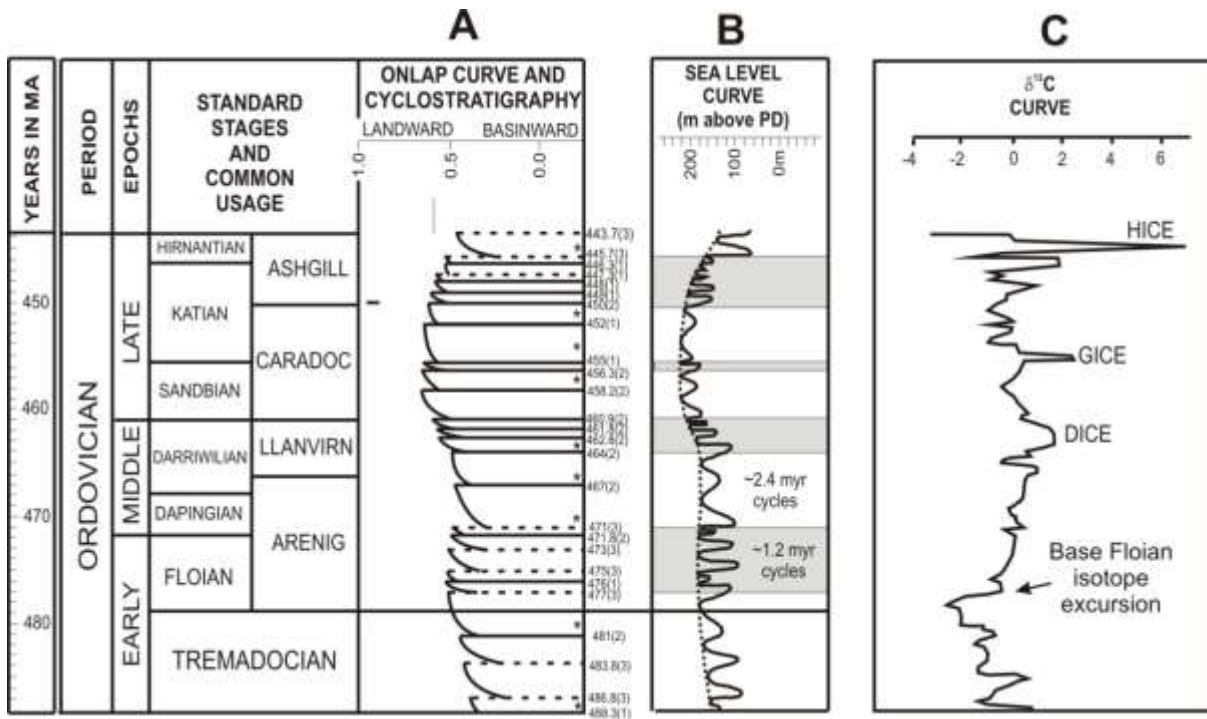
763

764

765

766 Figure 5

767



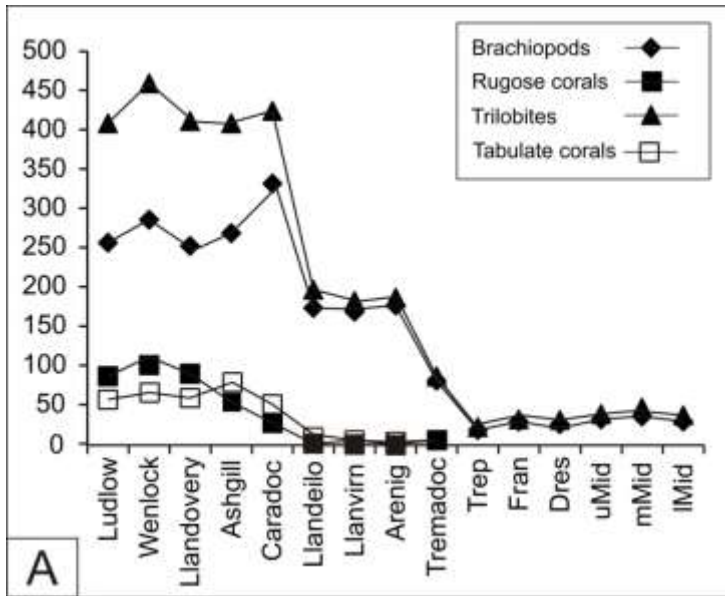
768

769

770 Figure 6

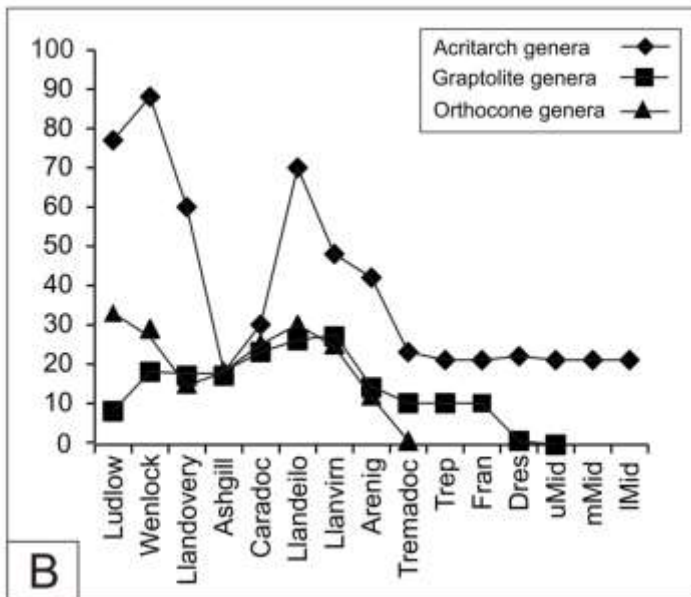
771

772



A

B



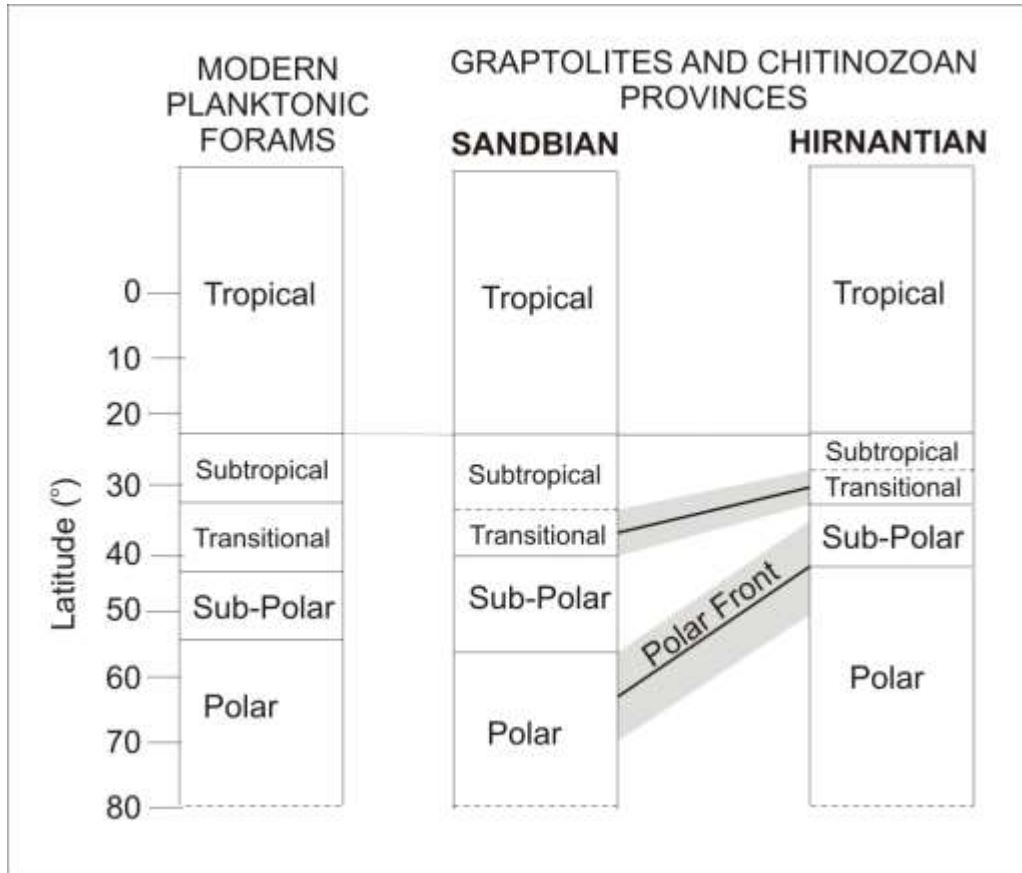
773

774

775

776

777



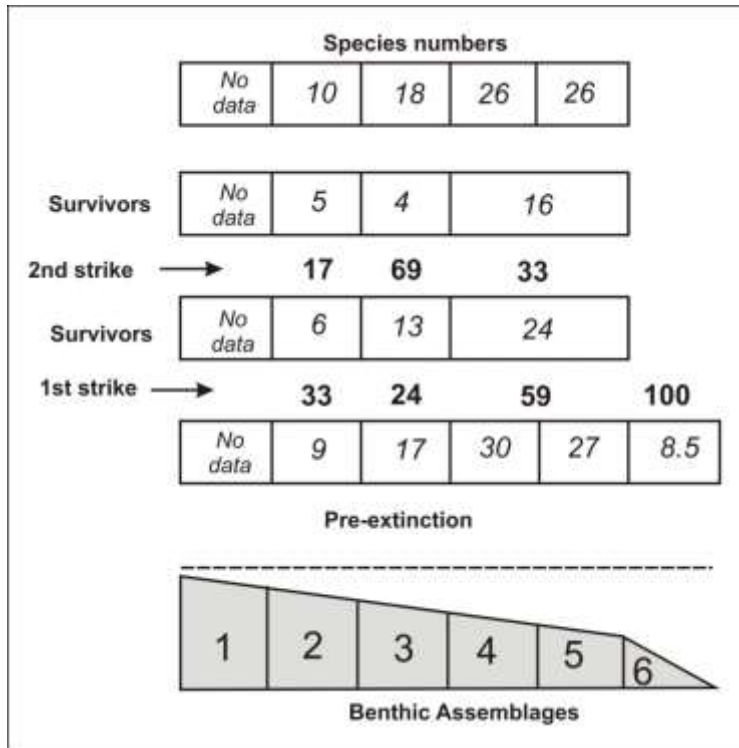
779

780

781 Figure 8

782

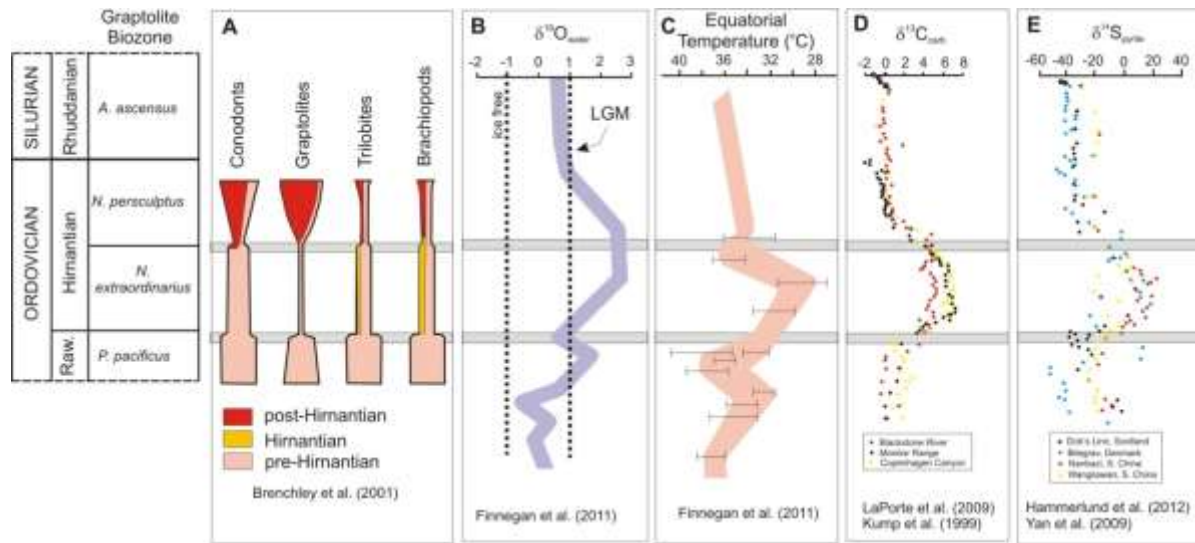
783



784

785

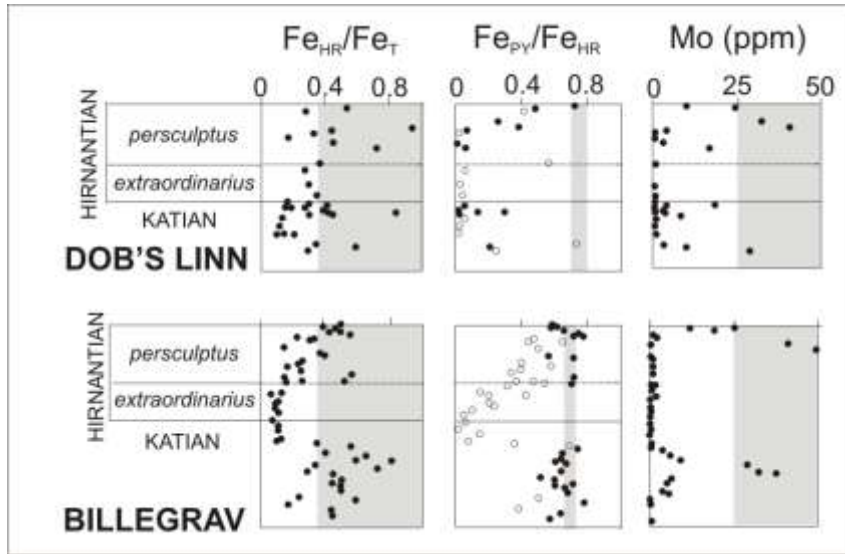
786 Figure 9



787

788

789 Figure 10.

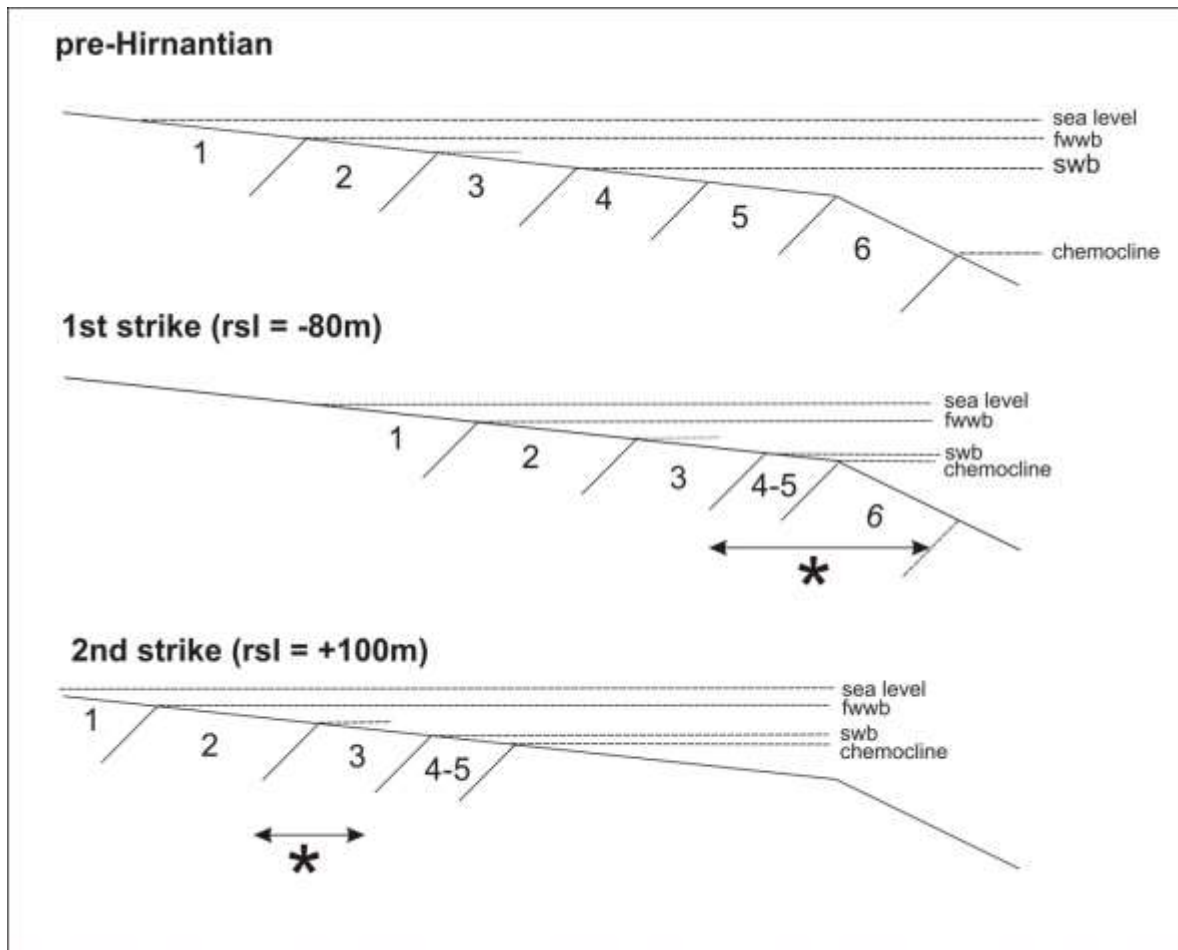


790

791

792 Figure 11

793



794

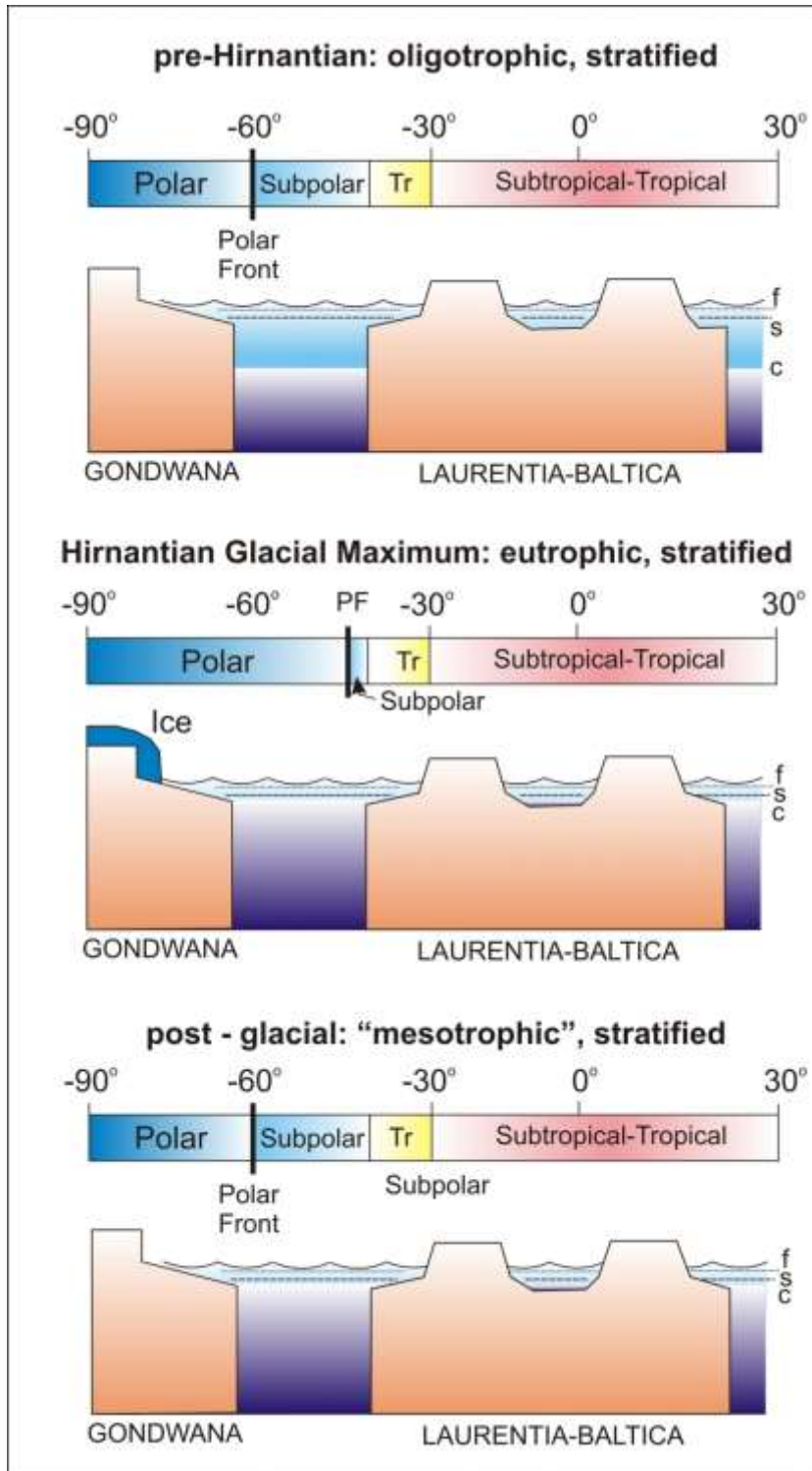
795

796

797 Figure 12

798

799



800

801
802
803
804
805